# Structure transforming for constructing constraint force field in musculoskeletal robot

*Shanlin Zhong*
Institute of Automation, Chinese Academy of Sciences, Beijing, China
*Ziyu Chen*
Institute of Automation, Chinese Academy of Sciences, Beijing, China, and Department of Automation, University of Science and Technology of China, Hefei, China, and
*Junjie Zhou*
Institute of Automation, Chinese Academy of Sciences, Beijing, China

**Abstract**

**Purpose** – Human-like musculoskeletal robots can fulfill flexible movement and manipulation with the help of multi joints and actuators. However, in general, sophisticated structures, accurate sensors and well-designed control are all necessary for a musculoskeletal robot to achieve high-precision movement. How to realize the reliable and accurate movement of the robot under the condition of limited sensing and control accuracy is still a bottleneck problem. This paper aims to improve the movement performance of musculoskeletal system by bio-inspired method.

**Design/methodology/approach** – Inspired by two kinds of natural constraints, the convergent force field found in neuroscience and attractive region in the environment found in information science, the authors proposed a structure transforming optimization algorithm for constructing constraint force field in musculoskeletal robots. Due to the characteristics of rigid-flexible coupling and variable structures, a constraint force field can be constructed in the task space of the musculoskeletal robot by optimizing the arrangement of muscles.

**Findings** – With the help of the constraint force field, the robot can complete precise and robust movement with constant control signals, which brings in the possibility to reduce the requirement of sensing feedback during the motion control of the robot. Experiments are conducted on a musculoskeletal model to evaluate the performance of the proposed method in movement accuracy, noise robustness and structure sensitivity.

**Originality/value** – A novel concept, constraint force field, is proposed to realize high-precision movements of musculoskeletal robots. It provides a new theoretical basis for improving the performance of robotic manipulation such as assembly and grasping under the condition that the accuracy of control and sensory are limited.

**Keywords** High precision, Attractive region in environment, Constraint force field, Musculoskeletal robot

**Paper type** Research paper

## 1. Introduction

Since the first industrial robot came online in 1962, more and more robot systems have entered the industrial production line, replacing workers to complete the repetitive, dangerous and heavy-load work, continuously creating remarkable production benefits for manufacturing enterprises (Peng *et al.*, 2021; Huang *et al.*, 2021). With the development of information science and mechanical engineering, robots are expected to be applied in a wider range of fields, such as high precision manufacturing (Huang *et al.*, 2020), military mission (Shen *et al.*, 2021) and medical service (Wang *et al.*, 2021), which puts forward higher requirements for robots to achieve high precision and dexterous operation in complex and unstructured scenes. However, the versatility of the robot at present is still far from approaching people's expectations.

As a comparison, the motor system of organisms in nature possesses extraordinary movement capacity. The rigid-flexible coupling characteristic of the musculoskeletal robot guarantees the dexterity of movement and the redundancy of degree of freedom (DOF) lays the foundation of the versatility of biological systems – the ability to complete a variety of tasks in dynamic and complex environments. Therefore, how to improve the performance of robots by referring to the superior characteristics of biological motion systems has become an essential research field.

However, introducing biological characteristics into robots is not straightforward. Although versatility is guaranteed, the redundancy of the musculoskeletal robot also brings in complex computational problems. Due to the number of DOFs

The current issue and full text archive of this journal is available on Emerald Insight at: **https://www.emerald.com/insight/0144-5154.htm**

Assembly Automation

[DOI 10.1108/AA-07-2021-0093]

The authors would like to thank Wei Wu, Erlong Kang for their help in discussions. This work is supported by The National Key Research and Development Program of China (2017YFB1300200, 2017YFB1300203), the National Natural Science Foundation of China (under grant 61627808, 91648205, 91948303), the Strategic Priority Research Program of the Chinese Academy of Science under grant XDB32050100.

Received 14 July 2021
Revised 7 October 2021
31 October 2021
Accepted 9 November 2021

of the musculoskeletal robot being much larger than that needed for action, the control patterns recruited for a given motion are infinite in theory, leading to an "ill-posed" computational problem. As a preliminary exploration, some research works have been conducted to solve the control problem of the musculoskeletal system with redundant actuators. Dong *et al.* put forward an efficient muscle coordination method to adaptively distribute the load throughout the muscles (Dong *et al.*, 2015). The method is able to keep high computational efficiency with the increase of muscle number. Chen *et al.* proposed a muscle synergy-based controller to realize human-like manipulation in a musculoskeletal system (Chen *et al.*, 2019). Huang *et al.* combined the mechanism of emotion modulation to the learning process of a recurrent neural network, which improves the motion learning performance of a musculoskeletal model in reaching tasks (Huang *et al.*, 2018).

In comparison, organisms have an inborn talent for efficiently coping with such problems. A newborn wildebeest is able to walk shortly after birth and the spinal cord of a headless frog can organize complex trajectories and rapidly correct for perturbations (Hart and Giszter, 2010; Kargo and Giszter, 2000a). These remarkable motion abilities mainly benefit from the well-developed regulatory mechanisms of the brain, as well as the synergies of the spinal cord and muscles. But how the motor system settles such complex computational problems is still a matter of concern.

Many neuronal circuitries and mechanisms underlying motion control have been proposed in previous research (Chen and Qiao, 2020; Qiao *et al.*, 2021). Some perspectives believed that to generate voluntary movements in different conditions, the central nervous system not only relies on the complex computation in the neuron system in the brain but also takes full advantage of the biomechanical properties of the limb, such as the mechanical properties of the muscles and the spatial organization of the circuits of the spinal cord (Bizzi *et al.*, 1991). For example, Elwood Henneman proposed the recruitment principle of motorneurons during movement, which is known as the Henneman Size Principle (Liggett *et al.*, 2010). This principle proposed that at the early stage of the movement, muscles with low innervation ratio are first recruited to provide small but enduring force, while the muscles with high innervation ratio are recruited later to provide explosive but transient force, so as to maintain the stability of posture and variety of movement. Another typical example is knee-jerk reactions (Michael *et al.*, 2009). When a muscle is disturbed by an external disturbance and causes an unexpected change in length, alpha motor neurons that originate from the spinal cord will generate a signal to activate the muscle to quickly regain its original length. This mechanism helps humans maintain the stability of their limbs when unexpected disturbances occur.

One of the most attractive ideas is the equilibrium point hypothesis (Bizzi *et al.*, 1991; Giszter *et al.*, 1993). This hypothesis describes that the microstimulation at a particular interneuronal zone in the spinal cord will elicit force of limb, whose direction and magnitude are differed depending on the position of the limb in space and there is a particular point, called equilibrium point, that the force vectors converged on it and the force elicited at it was zero (Georgopoulos, 1994). Experiments performed in surgically altered frogs have provided neurophysiological evidence for the equilibrium point hypothesis. Specifically, in the experiment, the spinal cord of the frog was first disconnected from the brainstem by surgery. The isometric forces generated by muscles of the leg at different ankle locations were measured when subjected to the same spinal micro-stimulation. The spatial distribution of the isometric forces generated by the micro-stimulation presented a well-defined pattern, called convergent force field, which was characterized by a single equilibrium point to which the force vectors converged. The equilibrium point indicated the position at which the leg of the experimental frog would be at a steady-state if it were free to move. These experimental results have suggested that the spinal circuitry can produce precisely balanced contractions in groups of muscles when it was activated. The limb was directed toward an equilibrium point in space with the forces generated by synergistic contractions of muscles (Bizzi *et al.*, 1998).

The equilibrium point hypothesis was thought to be significant for the control of voluntary movements (Bizzi *et al.*, 1991). The cooperation of muscle's elastic properties and activation of spinal circuitry internalize as the intrinsic characteristics of the motion system, which can help the brain enhance the understanding of the body itself. Research on the movement of a single joint demonstrated that the formation of arm trajectories with moderate velocities is able to be completed by specifying a series of equilibrium positions of the limb (Bizzi *et al.*, 1982). By analyzing trajectory correction responses during hindlimb wiping in spinal frogs, William and Simon confirmed that the vector summation of force-field primitives can produce a large range of dynamic force-field structures associated with limb behaviors (Kargo and Giszter, 2000b). Corey B. Hart *et al.* verified that dedicated sets of interneurons of the spinal cord relate significantly better to the spinal motor primitives than to the activation of the individual muscles (Hart and Giszter, 2010).

The hypothesis of force field with equilibrium point is similar to previous research in attractive region in environment (ARIE). The ARIE is an innovative concept for realizing high-precision manipulation with a low-precision system, which is initially proposed by Qiao (2000). It is a kind of constrained region formed by the environment in the configuration space of the robotic system, from any point of which the uncertainty of the system can be eliminated by a state-independent input (Qiao *et al.*, 2015). The concept of ARIE can be easily understood by the example of a bean-bowl system. Imagine there is a bean in a bowl. No matter where the initial position of the bean is, it will always drop into the bowl and finally stay at the bottom of the bowl under the effect of gravity and friction. Suppose the bean represents the state of the system and the bowl represents the environmental constraints, if there is a state-independent input, such as gravity, can drive the state of the system converging to a stable state in the "bowl," then such a "bowl" is called the ARIE. Inspired by this physical phenomenon, the concept of ARIE provides a theoretical foundation for realizing high-precision manipulation with a low-precision system (Li and Qiao, 2019). Su *et al.* proposed a strategy based on the ARIE for the assembly of an unfixed piston-peg-rod of an automotive engine with a tolerance of approximately 2–7.5 $\mu$m (Su *et al.*, 2012). With the help of the ARIE, Matteo Gilli *et al.* used Barrett Technology's WAM Arm, a 7 DOF robotic manipulator with repeatability of 2 mm,

to complete a peg-in-hole insertion task with an accuracy of 0.21 mm (Gilli *et al.*, 2014). Li *et al.* proposed a learning-based ARIE to realize robust form-closure grasping planning with a 4-pin gripper (Li *et al.*, 2020).

Based on the research results from the fields of neuroscience and information science, we found that the convergent force field of muscle and attractive region in the environment are very similar: they all have a certain stable point of the system state and the system can converge to the stable point with state-independent control inputs. Therefore, how to find a similar constraint field in musculoskeletal robots and further leverage it to achieve robust and accurate movement becomes the focus of this paper.

In this work, inspired by the two kinds of natural constraints, the convergent force field found in neuroscience and attractive region in the environment found in information science, we proposed a structure transforming optimization algorithm for constructing a new kind of constraint in musculoskeletal robots, called constraint force field (CFF). For the musculoskeletal robotic system with rigid-flexible coupling and variable structures, by optimizing the arrangements of muscles, a CFF can be constructed at any specified position in the task space, which can help the robot to complete precise and robust movement with constant control signals. The leverage of the CFF brings in the possibility to reduce the requirement of sensing feedback during the motion control of the robot. The main contributions of this paper are listed as follows.

- The dynamic model of the musculoskeletal robot with the variable arrangement of muscles is built. To describe the structure variation of the musculoskeletal model, the attachment points of muscles on the skeletons are set as independent variables. With the variation of the position of attachment points, the functions of muscle length, muscle force and muscle torque are given.
- A structure-transforming optimization algorithm for constructing CFF in the task space of the musculoskeletal robot is proposed. Based on the dynamic model of the musculoskeletal robot with variable arrangements of muscles, a nonlinear-constrained optimization problem about the force field formed by the terminal force of the robot is constructed. By solving the optimization problem, optimal arrangements of muscles could be found to construct a CFF, which can help the robot accurately move to the specified position with constant control signals.
- The effectiveness of the CFF is verified by theoretical proof and simulation experiments. The motion stability of the musculoskeletal robot in the CFF is proved based on the Lyapunov stability theorem. A musculoskeletal model with 2 DOFs and 4 muscles is used to verify the wide existence of the CFF in the task space of the system. The effectiveness of the CFF in improving movement accuracy and robustness to control noise is validated. The sensitivity of the CFF to structure precision is discussed.

The rest of this paper is organized as follows. The theory and algorithm to construct CFF in musculoskeletal robotic systems are introduced in Section 2. The effectiveness of the proposed method is analyzed in Section 3. Section 4 presents the experimental results to demonstrate the performance of the proposed method. Conclusion and future work are introduced in Section 5.

## 2. Construction of constraint force field

### 2.1 Dynamics of the musculoskeletal model with variable muscles

The main difference between the human motor system and the traditional robot is that it uses highly redundant and flexible muscles as actuators. Muscles provide forces for maintaining posture and generating free movement of the body. Stable posture is achieved by the balance of competing forces between the muscles, while free movement is produced by the imbalance of muscle forces.

To simulate the musculoskeletal model accurately, the modeling precision of the biological muscle unit is essential. In this paper, we use a Hill-type model, which is widely used in biomechanics research, to simulate the biomechanical characteristics of human muscle (Millard *et al.*, 2013). The Hill-type model uses a contractile element (CE) and a passive elastic element (PE) to mimic the muscle fiber. CE and PE are connected in parallel. CE is adopted to mimic sarcomere composed of actin and myosin. It can contract to produce active force in response to neural activation. PE is an elastic element, which is used to mimic the non-contractile tissue composed of structural proteins and extracellular connective tissue. The muscle fiber is a basic structural unit of muscle. It is the source of active force for the movement of the skeleton system.

The active force produced by muscle fiber is mainly dependent on the amplitude of activation $a$, muscle fiber length $l^{ce}$ and contraction velocity $v^{ce}$. In neurophysiological experiments, the convergent force field of muscle is composed of the terminal force of limbs that is generated by isometric contraction of the muscle under the constant microcurrent stimulation. It means that the activation of muscle $a$ is constant and the contraction velocity $v^{ce}$ is 0. So the active force generated by muscle fiber is only related to the muscle fiber length $l^{ce}$.

Suppose the musculoskeletal system has $M$ muscles. Muscle $i$ has $N_i$ attachment points on the skeleton. Let $l_{ij}$ denote the coordinate value of the $j$th attachment point of muscle $i$ in the reference frame of the skeleton that it attaches to. We use $\mathbf{L} = \{l_{11}, \ldots, l_{1N_1}, \ldots, l_{i1} \ldots, l_{iN_i}, \ldots, l_{MN_M}\}$ it to represent the coordinate set of all attachment points of the musculoskeletal system. Based on the coordinate transformation relationship between joints defined by kinematics, $l_{ij}$ can be converted to the coordinate representation in the world frame of the robot system. The coordinate value in the world frame is denoted as ${}^{w}l_{ij}$. Thus, the length of muscle fiber w.r.t variable arrangements $\boldsymbol{L}$ is defined as the summation of distances between all attachment points of muscle $i$:

$$l_i(\mathbf{L}) = \sum_{j=1}^{N_{i-1}} \sqrt{\left({}^{w}l_{ij} - {}^{w}l_{i(j+1)}\right)^T \left({}^{w}l_{ij} - {}^{w}l_{i(j+1)}\right)}. \quad (1)$$

Let $l_0^{m_i}$ denote the optimal fiber length of muscle $i$ and $f_0^{m_i}$ denote its maximum isometric force. The biological meaning of $f_0^{m_i}$ is the maximum force that muscle $i$ can generate by isometric contraction in length $l_0^{m_i}$. The value of $l_0^{m_i}$ and $f_0^{m_i}$ are set according to the biomechanical parameters measured in

physiological experiments (Holzbaur *et al.*, 2005). Then, the definition of normalized muscle fiber length is given as follow:

$$\tilde{l}_i(\mathbf{L}) = \frac{l_i(\mathbf{L})}{l_0^{m_i}}. \tag{2}$$

The active force operator is modeled by an exponential function (Millard *et al.*, 2013; Holzbaur *et al.*, 2005; Zhong *et al.*, 2019):

$$f_i^{ce}\left(\tilde{l}_i(\mathbf{L})\right) = \exp\left(-2\left(\tilde{l}_i(\mathbf{L}) - 1\right)^2\right). \tag{3}$$

The passive force operator is modeled by a piecewise function (Millard *et al.*, 2013; Holzbaur *et al.*, 2005; Zhong *et al.*, 2019):

$$f_i^{pe}\left(\tilde{l}_i(\mathbf{L})\right) = \begin{cases} 1 + \dfrac{k^{pe}}{\varepsilon_0^m}\left[\tilde{l}_i(\mathbf{L}) - \left(1 + \varepsilon_0^m\right)\right], & \tilde{l}_i(\mathbf{L}) > 1 + \varepsilon_0^m \\ \dfrac{\exp\left(k^{pe}\left(\tilde{l}_i(\mathbf{L}) - 1\right)/\varepsilon_0^m\right)}{\exp(k^{pe})}, & \tilde{l}_i(\mathbf{L}) \le 1 + \varepsilon_0^m \end{cases} \tag{4}$$

where $k^{pe} = 0.5$ is an exponential shape factor and $\varepsilon_0^m = 0.6$ is the passive muscle strain due to maximum isometric force.

With a constant activation $a^*$ and muscle arrangements $\boldsymbol{L}$, muscle force can be represented as the summation of active force and passive force:

$$F_i\left(\tilde{l}_i(\mathbf{L}), a^*\right) = f_0^{m_i}\left[a^* \cdot f_i^{ce}\left(\tilde{l}_i(\mathbf{L})\right) + f_i^{pe}\left(\tilde{l}_i(\mathbf{L})\right)\right] \tag{5}$$

With the movement of joints, moment arms of muscles to the joints are changing. The moment arm converts the force generated by muscles into the rotational torque of the joint. It plays an important role in determining the change of muscle length during joint rotation, which will affect the amplitude of muscle force as in (5). The method to calculate the moment arm is proposed in our previous work (Zhong *et al.*, 2019). Let $R_{ji}(\mathbf{L}, \alpha_j)$ represent the moment arm of muscle $i$ to joint $j$, where $\alpha_j$ is the joint angle. The torque generated by each muscle can be expressed by the product of the muscle force and its moment arm to the joint. Let $\tau_j$ represent the resultant torque provided by all muscles in the robot for joint $j$. Then $\tau_j$ can be solved by calculating the summation of torque generated by each muscle, which is formulated as follows:

$$\tau_j\left(\mathbf{L}, a^*, \alpha_j\right) = \sum_{i=1}^{M} R_{ji}(\mathbf{L}, \alpha_j) \cdot F_i\left(\tilde{l}_i(\mathbf{L}), a^*\right) \tag{6}$$

Based on the dynamics of the rigid body, the dynamics of the musculoskeletal robot with variable arrangements $\boldsymbol{L}$ can be formulated as follows:

$$\boldsymbol{\Gamma}(\mathbf{L}, \mathbf{a}^*, \boldsymbol{\alpha}) = \mathbf{M}(\boldsymbol{\alpha})\,\ddot{\boldsymbol{\alpha}} + \mathbf{C}_c(\boldsymbol{\alpha}, \boldsymbol{\alpha}.)\,\boldsymbol{\alpha}. + \mathbf{b}(\boldsymbol{\alpha}.) + \mathbf{G}(\boldsymbol{\alpha}) + \tau_f \tag{7}$$

where $\boldsymbol{\Gamma}(\mathbf{L}, \mathbf{a}^*, \boldsymbol{\alpha}) = \{\tau_1(\mathbf{L}, a^*, \alpha_1), \ldots, \tau_K(\mathbf{L}, a^*, \alpha_K)\}$ is the joint torque vector of the musculoskeletal robot, whose values are dependent on the arrangements of muscles $\boldsymbol{L}$, the vector of constant activations $\mathbf{a}^*$ and the vector of joint angle $\boldsymbol{\alpha}$. $K$ is the number of joints. $\boldsymbol{\alpha}.$ and $\boldsymbol{\alpha}..$ are angular velocity and acceleration of joint, respectively. $\mathbf{M}(\boldsymbol{\alpha})$ is the mass matrix of the skeleton model. $\mathbf{C}_c(\boldsymbol{\alpha}, \boldsymbol{\alpha}.)$ is the Coriolis force matrix. $\mathbf{b}(\boldsymbol{\alpha}.)$ is the damping term. $\mathbf{G}(\boldsymbol{\alpha})$ is the gravity vector. $\tau_f$ is the friction torque of the joints.

### 2.2 Constructing constraint force field by structure transforming optimization

Traditional articulated robots have fixed body structures. They rely on precise assembly and tight coordination of all parts, such as servo motor, harmonic reducer and gearbox, to realize high-precision movement. Compared with articulated robots, the muscle actuators of the musculoskeletal robot have advantages in lightweight, flexibility and variable arrangements, which provides a structural basis for exploring how to improve the performance of robots by optimizing the structure. Based on the dynamics of the musculoskeletal model with variable muscles, in this part, we propose a structure-transforming optimization algorithm to find and construct CFF in the task space of the system.

Similar to the convergent force field of muscle found in neuroscience, for constructing CFF in the musculoskeletal robotic system, we first need to convert the joint torque provided by muscles to the equivalent terminal force of the robot. Let $\boldsymbol{J}$ denote the Jacobian matrix of musculoskeletal robots in Cartesian coordinates. The element in the $i$th row and the $j$th column of $\boldsymbol{J}$ is solved by the following equation:

$$\mathbf{J}_{ij}(\hat{\boldsymbol{\alpha}}(\mathbf{r})) = \frac{\partial x_i(\hat{\boldsymbol{\alpha}}(\mathbf{r}))}{\partial}\hat{\alpha}_j,\ i = 1, \ldots, D; j = 1, \ldots, K \tag{8}$$

where $D$ is the movement dimension of the robot. $\boldsymbol{r}$ represents the target position of the terminal point of the robot in Cartesian coordinates. $x_i(\hat{\boldsymbol{\alpha}}(\mathbf{r}))$ is the $i$th dimension of the Cartesian coordinate. $\hat{\boldsymbol{\alpha}}(\mathbf{r})$ denotes the joint vector corresponding to target position $\boldsymbol{r}$, which can be solved by inverse kinematics of the robot. Then, the inverse matrix of transpose Jacobian matrix can be expressed as follows:

$$\mathbf{A}(\mathbf{r}) = \mathbf{J}(\hat{\boldsymbol{\alpha}}(\mathbf{r}))^{-T} \tag{9}$$

By multiplying $\mathbf{A}(\mathbf{r})$ and joint torque $\boldsymbol{\Gamma}(\mathbf{L}, \mathbf{a}^*, \boldsymbol{\alpha})$, we can obtain the equivalent terminal force of the robot with constant muscle activations $\mathbf{a}^*$, which can be formulated as follows:

$$Q(\mathbf{L}, \mathbf{r}, \mathbf{a}^*) = \mathbf{A}(\mathbf{r})\boldsymbol{\Gamma}(\mathbf{L}, \mathbf{a}^*, \hat{\boldsymbol{\alpha}}(\mathbf{r})) = \begin{pmatrix} \sum_{j=1}^{K} A_{1j}(\mathbf{r})\tau_j(\mathbf{L}, \mathbf{a}^*) \\ \vdots \\ \sum_{j=1}^{K} A_{Dj}(\mathbf{r})\tau_j(\mathbf{L}, \mathbf{a}^*) \end{pmatrix} \tag{10}$$

where $A_{ij}(\mathbf{r})$ is the element of the $i$th row and the $j$th column in the matrix $\mathbf{A}(\mathbf{r})$. Obviously, given a specific movement target $\boldsymbol{r}$ and activation pattern $\mathbf{a}^*$, (10) only relates to the arrangements of muscles $\boldsymbol{L}$, so it can be abbreviated as $Q(\mathbf{L})$.

According to (10), the terminal force $Q(\mathbf{L})$ at different positions in the task space of the robot can be changed by

adjusting the arrangements of muscles $\boldsymbol{L}$. Therefore, for any specified target position $\mathbf{r}_T$ in the task space, by optimizing the muscles' arrangements $\boldsymbol{L}$, a CFF with $\mathbf{r}_T$ as the equilibrium center can be constructed, which is able to help the robot to accurately move to the target position $\mathbf{r}_T$.

To solve the optimal muscle arrangements $\mathbf{L}_{opt}$ for constructing CFF in the musculoskeletal robot, a nonlinear-constrained optimization problem is established as follows:

$$\begin{aligned} &\min_{\mathbf{L}} W = \lambda_1 \cdot Q(\mathbf{L})^T Q(\mathbf{L}) \\ &\quad + \lambda_2 \cdot \sum_{i=1}^{G} \mathcal{H}\left(\theta\left(\mathbf{c}_i(\mathbf{r}_T, \mathbf{r}_i), \mathbf{f}_i(\mathbf{L}, \mathbf{r}_i, \mathbf{a}^*)\right)\right) \\ &s.t. \quad \mathbf{L}_l \le \mathbf{L} \le \mathbf{L}_u \end{aligned} \tag{11}$$

where $\lambda_1$ and $\lambda_2$ are penalty factors for balancing the importance of the two optimization term. $[\mathbf{L}_l, \mathbf{L}_u]$ is the position range of the attachment points. $G$ is the number of neighborhood points of $\mathbf{r}_T$. The neighborhood points are equidistantly selected from a circle with center $\mathbf{r}_T$ and radius $\varepsilon > 0$. $\mathbf{c}_i(\mathbf{r}_T, \mathbf{r}_i)$ represents the unit vector that points to $\mathbf{r}_T$ from neighborhood point $\mathbf{r}_i$. The formula for calculating $\mathbf{c}_i(\mathbf{r}_T, \mathbf{r}_i)$ is:

$$\mathbf{c}_i(\mathbf{r}_T, \mathbf{r}_i) = \frac{\mathbf{r}_T - \mathbf{r}_i}{|\mathbf{r}_T - \mathbf{r}_i|} \tag{12}$$

where $|\cdot|$ is the magnitude of a vector. $\mathbf{f}_i(\mathbf{L}, \mathbf{r}_i, \mathbf{a}^*)$ is the unit vector of the robot's terminal force $Q(\mathbf{L}, \mathbf{r}_i, \mathbf{a}^*)$ at the neighborhood point $\mathbf{r}_i$. The formula for calculating $\mathbf{f}_i(\mathbf{L}, \mathbf{r}_i, \mathbf{a}^*)$ is:

$$\mathbf{f}_i(\mathbf{L}, \mathbf{r}_i, \mathbf{a}^*) = \frac{Q(\mathbf{L}, \mathbf{r}_i, \mathbf{a}^*)}{|Q(\mathbf{L}, \mathbf{r}_i, \mathbf{a}^*)|} \tag{13}$$

$\mathbf{c}_i(\mathbf{r}_T, \mathbf{r}_i)$ and $\mathbf{f}_i(\mathbf{L}, \mathbf{r}_i, \mathbf{a}^*)$ can be abbreviated as $\mathbf{c}_i$ and $\mathbf{f}_i$, respectively. Let $\theta(\mathbf{c}_i, \mathbf{f}_i)$ represent the angle between the vector $\mathbf{c}_i$ and $\mathbf{f}_i$. The penalty function $\mathcal{H}(\cdot)$ in (11) is designed to constrain the direction of terminal forces at the neighborhood points. It requires the terminal forces at the neighborhood points contain a force component pointing to the target point, so as to form a convergent CFF. A hyperbolic cosine function is applied to construct $\mathcal{H}(\cdot)$, which is formulated as follows:

$$\mathcal{H}(\theta(\mathbf{c}_i, \mathbf{f}_i)) = \beta^2 \left( cosh\left( \frac{cos(\theta(\mathbf{c}_i, \mathbf{f}_i)) - 1}{\beta} \right) - 1 \right) \tag{14}$$

where $cosh(x) = (e^x - e^{-x})/2$. The penalty range of $\mathcal{H}(\cdot)$ is dependent on parameter $\beta$. As the optimization object is to make $\theta(\mathbf{c}_i, \mathbf{f}_i)$ as small as possible, so the value of $\beta$ should make the function $\mathcal{H}(\theta(\mathbf{c}_i, \mathbf{f}_i))$ pay a high cost in $cos(\theta(\mathbf{c}_i, \mathbf{f}_i)) \in [-1, 0]$, while in $cos(\theta(\mathbf{c}_i, \mathbf{f}_i)) \in [0, 1]$ the cost is low. The effect of $\mathcal{H}(\theta(\mathbf{c}_i, \mathbf{f}_i))$ on optimization is shown in Figure 1.

To visualize the CFF optimized by (11), within a rectangular range with the center point $\mathbf{r}_T$ and side length $\varrho$, $S$ points are uniformly selected with stepsize $\delta$. Let $S_v$ denote the position set formed by the selected points. The terminal force of the robot $Q(\mathbf{L}, \mathbf{r}_s, \mathbf{a}^*)$ at the selected position $\mathbf{r}_s$ is normalized according to the following formula:

$$\tilde{Q}(\mathbf{r}_s) = \frac{\delta}{2} \cdot \frac{|Q(\mathbf{L}, \mathbf{r}_s, \mathbf{a}^*)|}{Q_{max}}, s = 1, \ldots, S \tag{15}$$

where $Q_{max}$ is the maximum terminal force of point in the position set $S_v$. In the CFF, the force vector at each position of $S_v$ is drawn in the direction of $Q(\mathbf{L}, \mathbf{r}_s, \mathbf{a}^*)$ and the length of $\tilde{Q}(\mathbf{r}_s)$. The CFF can be visualized as shown in Figure 2(a).

Similar to the convergent force field of muscle found in neuroscience, the CFF constructed in musculoskeletal robot mainly has two features:

1 The specified target position is the equilibrium center of the CFF. With constant muscle activations $\mathbf{a}^*$, the terminal force of the robot at the target position is 0, i.e. $Q(\mathbf{L}, \mathbf{r}_T, \mathbf{a}^*) = 0$.
2 The force vectors in the CFF converge to the equilibrium center. In a certain neighborhood of the target point $\mathbf{r}_T$, the terminal force of the robot at each position has a force component pointing to $\mathbf{r}_T$, thus forming a CFF with approximate centripetal convergence.

**Figure 1** The effect of $\mathcal{H}(\theta(\mathbf{c}_i, \mathbf{f}_i))$ on optimization

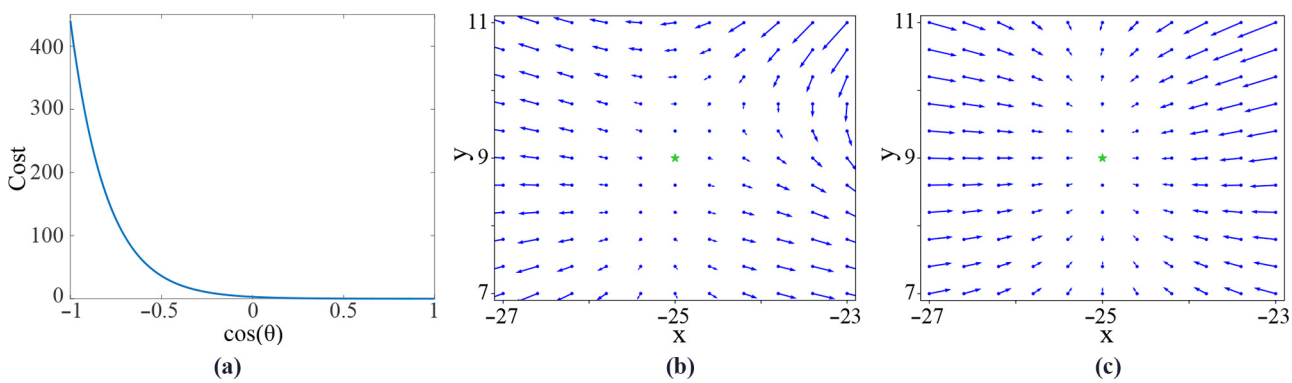


**Notes:** (a) The curve of $\mathcal{H}(\theta(\mathbf{c}_i, \mathbf{f}_i))$ when $\beta = 0.2$; (b) Without $\mathcal{H}(\theta(\mathbf{c}_i, \mathbf{f}_i))$ in the objective function (11), although the terminal force of the robot at the target position can be approximate to 0, it is difficult to ensure the convergence of the CFF; (c) After adding $\mathcal{H}(\theta(\mathbf{c}_i, \mathbf{f}_i))$, it is easier to find the optimal arrangements of muscles for constructing a convergent CFF

**Figure 2** Constraint force field formed by optimizing the muscle arrangements

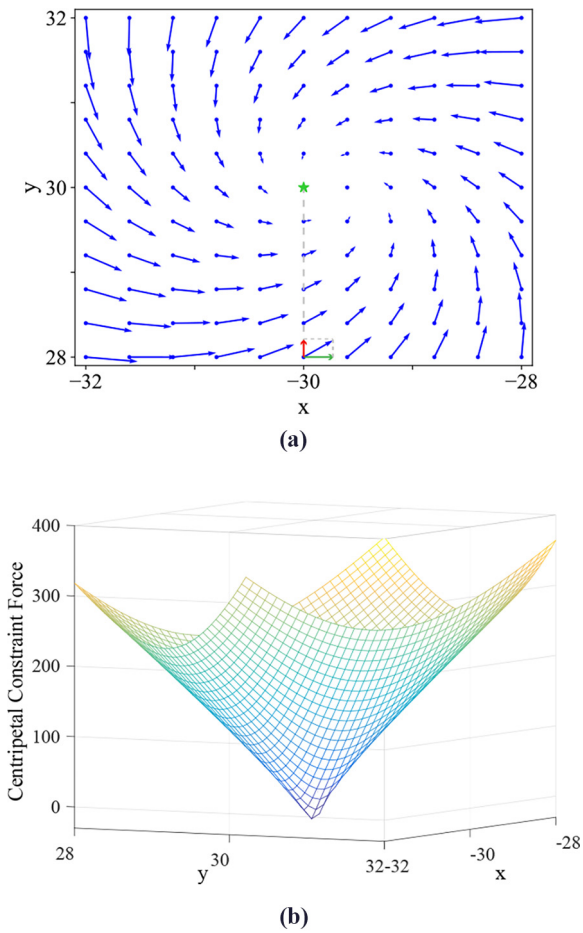


**Notes:** (a) The green star represents the target position rT. the blue arrow represents the normalized terminal force at the starting point of the arrow. The red arrow represents the force component pointing to the target position and the green arrow represents the vertical force component of the red arrow; (b) the centripetal constraint force field

For further analyzing the characteristics of the CFF, a new definition called centripetal constraint force is introduced. Centripetal constraint force represents the force component obtained by prejecting the terminal force of each point (i.e. $Q(\mathbf{L}, \mathbf{r}_s, \mathbf{a}^*)$) into the centripetal direction pointing to the target position. Let $Q_{c_s}(\mathbf{L}, \mathbf{r}_s, \mathbf{a}^*)$ denote the centripetal constraint force, which can be abbreviated as $Q_{c_s}$. The formula for computing $Q_{c_s}$ is:

$$Q_{c_s} = cos(\theta(\mathbf{c}_s, \mathbf{f}_s)) \cdot |Q(\mathbf{L}, \mathbf{r}_s, \mathbf{a}^*)| \tag{16}$$

According to (16), when there is a force component of $Q(\mathbf{L}, \mathbf{r}_s, \mathbf{a}^*)$ pointing to the target position $\mathbf{r}_T$, $Q_{c_s}$ is positive, otherwise $Q_{c_s}$ is negative. By drawing $\{(\mathbf{r}_s, Q_{c_s}) | s = 1, \ldots, S\}$, we find that the CFF optimized by (11) forms a constraint region with the target position $\mathbf{r}_T$ as the local minimum point, which is very similar to the ARIE found robotic manipulation, such as peg-in-hole assembly (Qiao *et al.*, 2015; Li and Qiao, 2019). We define this constraint region as a centripetal constraint force field (C-CFF), as shown in Figure 2(b).

The construction of CFF provides a new kind of attractive region for musculoskeletal robotic systems to realize high precision movement. By optimizing the arrangements of muscles, a CFF can be constructed in the task space of the musculoskeletal robot, which is able to help the robot accurately move to the specified target position with constant activations. It greatly reduces the requirements for the feedback of sensing information and the precision of control signals in the control process of the robot and provides a theoretical basis for realizing the high-precision movement of the robot with limited control and sensing accuracy. The schematic diagram of the algorithm is illustrated in Figure 3. The blue line represents the optimization process. The orange line represents that the robot with optimal muscle arrangement moves to the target position with constant activations.

## 3. Effectiveness analysis of the constraint force field

The CFF provides a new kind of method to control the movement of the musculoskeletal robot. In this part, based on Lyapunov stability theory, the condition for the robot to stably reach the target with the help of CFF is discussed.

To stabilize the system under the control based on the CFF, it is necessary to consider the effects of damping and joint friction on the system dynamics, so that the total energy of the system is in a state of continuous dissipation. Taking the movement of a musculoskeletal robot in a two-dimensional plane as an example, the proof of control stability is introduced as follows.

Assume $\mathbf{r}_e$ is the equilibrium position of the robot in the CFF. The joint vector $\boldsymbol{\alpha}(\mathbf{r}_e)$ corresponding to $\mathbf{r}_e$ can be solved by inverse kinematics. The dynamics of the system is formulated as follows:

$$\mathbf{M}(\boldsymbol{\alpha})\,\ddot{\boldsymbol{\alpha}} + \mathbf{C}_c(\boldsymbol{\alpha}, \dot{\boldsymbol{\alpha}})\,\dot{\boldsymbol{\alpha}} + \mathbf{b}(\dot{\boldsymbol{\alpha}}) + \tau_f = \boldsymbol{\Gamma}(\boldsymbol{\alpha}(\mathbf{r})) \tag{17}$$

where $\boldsymbol{\Gamma}(\boldsymbol{\alpha}(\mathbf{r}))$ is the joint torque at position $\boldsymbol{r}$. The damping term $\mathbf{b}(\dot{\boldsymbol{\alpha}})$ and friction torque of the joints $\tau_f$ satisfy that when $\boldsymbol{\alpha}. \neq 0$, $\dot{\boldsymbol{\alpha}}^T\mathbf{b}(\dot{\boldsymbol{\alpha}}) > 0$, $\dot{\boldsymbol{\alpha}}^T\tau_f > 0$.

The kinetic energy of the system is taken as the Lyapunov function:

$$V(\dot{\boldsymbol{\alpha}}) = \frac{1}{2}\dot{\boldsymbol{\alpha}}^T\mathbf{M}(\boldsymbol{\alpha})\,\dot{\boldsymbol{\alpha}} \tag{18}$$

whose derivative is:

$$\begin{aligned}
V(\dot{\boldsymbol{\alpha}}) &= \frac{1}{2}\dot{\boldsymbol{\alpha}}^T\dot{\mathbf{M}}(\boldsymbol{\alpha})\,\dot{\boldsymbol{\alpha}} + \frac{1}{2}\dot{\boldsymbol{\alpha}}^T\mathbf{M}(\boldsymbol{\alpha})\,\ddot{\boldsymbol{\alpha}} + \frac{1}{2}\ddot{\boldsymbol{\alpha}}^T\mathbf{M}(\boldsymbol{\alpha})\,\dot{\boldsymbol{\alpha}} \\
&= \frac{1}{2}\dot{\boldsymbol{\alpha}}^T\dot{\mathbf{M}}(\boldsymbol{\alpha})\,\dot{\boldsymbol{\alpha}} + \dot{\boldsymbol{\alpha}}^T\mathbf{M}(\boldsymbol{\alpha})\,\ddot{\boldsymbol{\alpha}} \\
&= \frac{1}{2}\dot{\boldsymbol{\alpha}}^T\dot{\mathbf{M}}(\boldsymbol{\alpha})\,\dot{\boldsymbol{\alpha}} + \dot{\boldsymbol{\alpha}}^T\left[\boldsymbol{\Gamma}(\boldsymbol{\alpha}(\mathbf{r})) - \mathbf{C}_c(\boldsymbol{\alpha}, \dot{\boldsymbol{\alpha}}) - \mathbf{b}(\dot{\boldsymbol{\alpha}}) - \tau_f\right] \\
&= \left[\frac{1}{2}\dot{\boldsymbol{\alpha}}^T\dot{\mathbf{M}}(\boldsymbol{\alpha})\,\dot{\boldsymbol{\alpha}} - \dot{\boldsymbol{\alpha}}^T\mathbf{C}_c(\boldsymbol{\alpha}, \dot{\boldsymbol{\alpha}})\right] \\
&\quad + \dot{\boldsymbol{\alpha}}^T\left[\boldsymbol{\Gamma}(\boldsymbol{\alpha}(\mathbf{r})) - \mathbf{b}(\dot{\boldsymbol{\alpha}}) - \tau_f\right] \\
&= \dot{\boldsymbol{\alpha}}^T\boldsymbol{\Gamma}(\boldsymbol{\alpha}(\mathbf{r})) - \boldsymbol{\alpha}.^T\mathbf{b}(\dot{\boldsymbol{\alpha}}) - \dot{\boldsymbol{\alpha}}^T\tau_f
\end{aligned} \tag{19}$$

According to the characteristics of the CFF, the constraint force decreases with the distance between the endpoint of the

**Figure 3** The schematic diagram of the algorithm

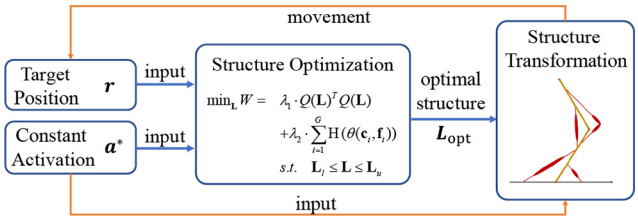


robot and the equilibrium position. Because of $\dot{\boldsymbol{\alpha}}^T\mathbf{b}(\dot{\boldsymbol{\alpha}}) > 0$ and $\dot{\boldsymbol{\alpha}}^T\boldsymbol{\tau}_f > 0$, there is an appropriate $\mathbf{b}(\dot{\boldsymbol{\alpha}})$ and $\boldsymbol{\tau}_f$ such that (19) is negative definite. When $\dot{\boldsymbol{\alpha}} = 0, \boldsymbol{\alpha}(\mathbf{r}) \to \boldsymbol{\alpha}(\mathbf{r}_e)$, the Coriolis force and damping term in the dynamics is 0, i.e. $\mathbf{C}_c(\boldsymbol{\alpha}, \dot{\boldsymbol{\alpha}}) = 0, \mathbf{b}(\dot{\boldsymbol{\alpha}}) = 0$. Then the dynamics of the robot can be written as follows:

$$\mathbf{M}(\boldsymbol{\alpha})\,\ddot{\boldsymbol{\alpha}} = \boldsymbol{\Gamma}(\boldsymbol{\alpha}(\mathbf{r})) - \boldsymbol{\tau}_f \tag{20}$$

So the robot will finally be stable in the range of $\boldsymbol{\Gamma}(\boldsymbol{\alpha}(\mathbf{r})) \le \boldsymbol{\tau}_f$. When $\boldsymbol{\tau}_f$ is small enough, the robot will reach the equilibrium position of the CFF accurately.

## 4. Experiments

### 4.1 Musculoskeletal model

Movement control of the musculoskeletal model is an intractable problem due to the strong nonlinearity of the muscle dynamics. In this paper, we proposed that by optimizing the arrangements of muscle to construct CFF, the musculoskeletal robot can realize high-precision movement with constant control signals, which is conducive to improving the movement performance of the robot with limited control and sensory accuracy. To verify the wide existence and effectiveness of the CFF, a musculoskeletal model with 2 DOFs and 4 muscles is used in our experiments.

The musculoskeletal model uses 4 Hill-type muscles as actuators, including Pectoralis Major (PECM), Deltoid (DELT), Biceps (BIC) and Triceps (TRI). The dynamics parameters of the muscle model, such as the optimal fiber length and the maximum isometric force, are set according to the biological parameters (Holzbaur *et al.*, 2005), as listed in Table 1.

The structure of the musculoskeletal model is depicted in Figure 4. $l_{ij}$ is the coordinate value of the $j$th attachment point of muscle $i$ in the reference frame of the skeleton that it attaches to. Especially, an additional attachment point in the TRI muscle is used to prevent the muscle from penetrating bone, where $l_{42} = 4$ and $\varphi = 2/3\pi$. The variable range of the position of the muscle attachment point is set as $[\mathbf{L}_l, \mathbf{L}_u] = [0, 30]$. The length of the links are $L_1 = L_2 = 30$ cm. The mass of each link is

**Figure 4** The musculoskeletal model with variable muscle arrangements

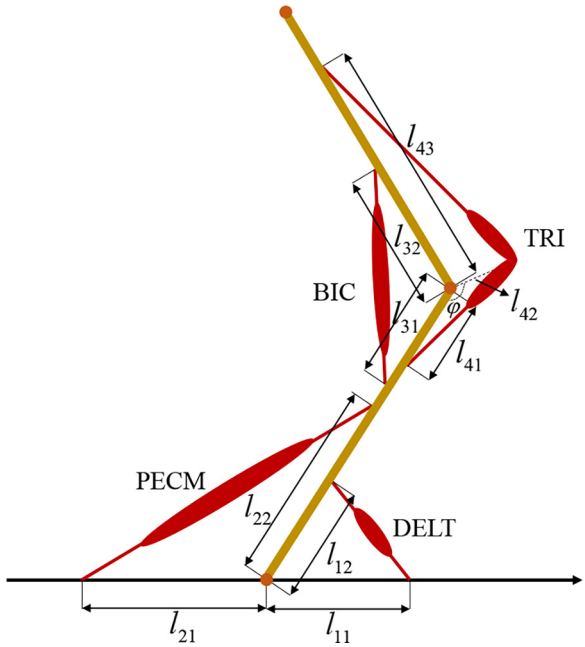


1 kg. The damping coefficient is 500 and the friction torque of the joint is 0.001. The range of joint motion is $[0, \pi]$. For parameters in the structure transforming optimization algorithm, the value of hyper-parameters $\lambda_1$ and $\lambda_2$ are, respectively, set to 10 and 1,000. The number of neighborhood points around the target position $G$ is set as 8, while the radius of the neighborhood $\varepsilon$ is 0.5. Parameter $\beta$ in the penalty function is 0.2. The constant activations $\mathbf{a}^*$ used in optimization are fixed in $\mathbf{1}$. The step size of the simulation is 0.01 and 4,000 steps are conducted in each experiment.

### 4.2 Movement accuracy evaluation

For any given target position in the task space of the musculoskeletal robotic system, by optimizing the muscle arrangements, a CFF with the given target as the equilibrium center can be constructed. When the initial state of the robot is within the CFF, the robot can accurately reach the target with constant activations used in optimization.

To demonstrate the effectiveness of CFF for motion control of the musculoskeletal robot, we randomly select 3 targets in the task space of the musculoskeletal robot and construct CFF with the specified target position as the equilibrium center by using the structure transforming optimization algorithm. In a $2 \times 2$ cm rectangle with the target as the center, $N_S = 100$ positions are randomly selected as the starting points of the

**Table 1** Parameters of muscles

| Muscle | Maximum isometric force (N) | Optimal fiber length (cm) | Tendon slack length (cm) |
|---|---|---|---|
| PECM | 515.4 | 13.8 | 8.9 |
| DELT | 1142.6 | 10.8 | 9.3 |
| BIC | 624.3 | 11.6 | 27.2 |
| TRI | 798.5 | 13.4 | 14.3 |

**Table 2** Optimal muscle arrangements

| $\mathbf{r}_T$ | $l_{11}$ | $l_{12}$ | $l_{21}$ | $l_{22}$ | $l_{31}$ | $l_{32}$ | $l_{41}$ | $l_{43}$ |
|---|---|---|---|---|---|---|---|---|
| **(−25,9)** | 5.6247 | 13.9283 | 13.1313 | 16.8818 | 3.5843 | 23.8212 | 0 | 14.4821 |
| **(−9,43)** | 18.2115 | 16.7706 | 15.6941 | 20.7743 | 20.3978 | 4.8036 | 0.2919 | 21.5759 |
| **(5,33)** | 12.0812 | 8.3911 | 8.2609 | 20.8856 | 1.9771 | 20.7219 | 3.2598 | 3.3599 |

**Table 3** Statistic index of movement accuracy

| $\mathbf{r}_T$ | Min PE (mm) | Max PE (mm) | Mean PE (mm) | Std PE (mm) |
|---|---|---|---|---|
| **(−25,9)** | 0.086 | 0.531 | 0.260 | 2.4e−4 |
| **(−9,43)** | 0.177 | 0.180 | 0.179 | 8.4e−4 |
| **(5,33)** | 0.073 | 0.074 | 0.074 | 3.6e−4 |

musculoskeletal robot. Note that the rectangle is within the CFF. The constant muscle activation used in optimization is $\mathbf{a}^* = 1$. Positioning error (PE), which is defined as the distance between the target position and the end-effector position of the robot at the end of the movement, is taken as the statistic index

**Figure 5** Experiments on the effectiveness of the CFF for improving movement performance of the musculoskeletal robot

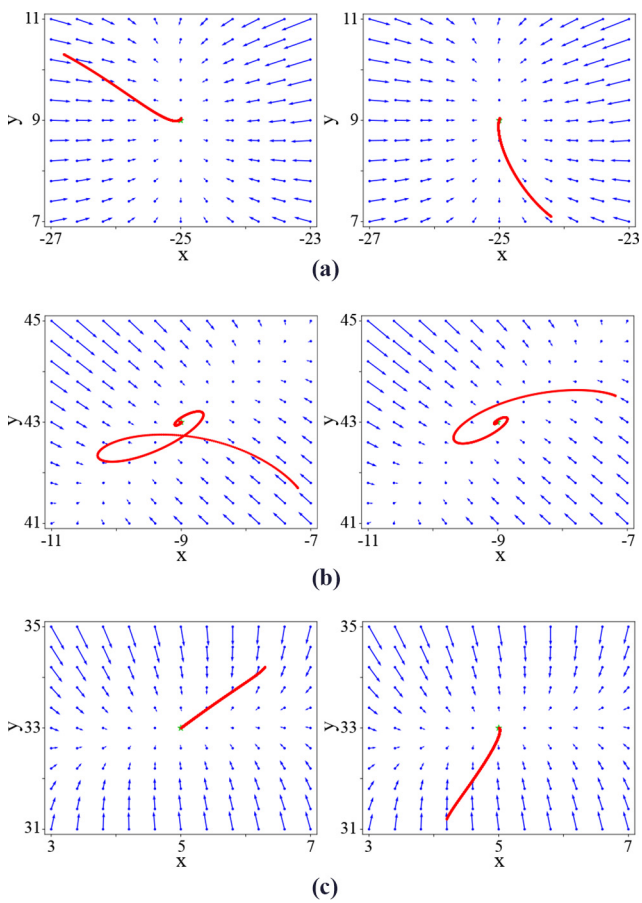


**Notes:** (a) $r_T = (-25,9)$; (b) $r_T = (-9,43)$; (c) $r_T = (5,33)$

to evaluate the movement accuracy. The experiment parameters and results can be found in Tables 2 and 3 and the movement trajectories of the robot in different CFF are depicted in Figure 5.

The experiment results demonstrate that starting from any position within the CFF, with the "guidance" of the constraint force, the musculoskeletal robot can accurately move to the target position with constant muscle activation. This process is very similar to the phenomenon that a bean drop into a bowl. Specifically, the effectiveness is mainly manifested in the following two aspects.

- The standard deviations (Std) of PE are very small. It means that for any movement in the same CFF, even if the starting point is different, the musculoskeletal robot can always accurately move to and stop at the equilibrium center of the CFF with the control of constant muscle activation.
- The mean values of PE are small. It means that the robot can reach the target position with high precision. There are two main reasons for the existence of motion error. Deviation exists in the position of the equilibrium center of the CFF and the desired target. In the optimization problem (11), the optimal solution is dependent on two optimization terms. The first term with parameter $\lambda_1$ requires that the terminal force at the target position tends to be zero. The purpose of this term is to make the equilibrium center of the CFF closes to the target position as much as possible. The second term with parameter $\lambda_2$ requires that the terminal forces at the neighborhood positions have force components pointing to the target. Optimizing these two terms at the same time is hard to guarantee that the $\lambda_1$ term strictly equals 0. So in some cases, the optimized equilibrium center of the CFF will be a bit deviating from the target point $\mathbf{r}_T$, which makes it become the main source of the movement error. The impact of the joint friction will influence the movement accuracy. According to (20), the final stable position of the system is impacted by the friction torque of the joints $\boldsymbol{\tau}_f$. So the decrease of joint friction can improve the movement accuracy of the system.

The experiment results reveal that the proposed method is beneficial for improving the motion performance of the robot

and simplifying the control strategy. It provides a foundation for a robot to realize high-precision movement with a simple control signal.

### 4.3 Noise robustness

A set of constant muscle activations $\mathbf{a}^*$ has to be specified before optimizing (11). The ideal CFF is formed when muscle structures are arranged according to the optimal structure $\mathbf{L}_{opt}$ and muscle activations are $\mathbf{a}^*$. So, when the control signals $\mathbf{a}^*$ are disturbed by noise, whether the motion of the robot in the CFF can still maintain a high precision? In this part, we discuss the noise robustness of the CFF.

The experiments are conducted in the CFF centered with $\mathbf{r}_T = (-25, 9)$. The constant muscle activations $\mathbf{a}^*$ used in optimization are fixed in $\mathbf{1}$. During the movement of the musculoskeletal robot in the CFF, the activation of the $i$th muscle at time $t$ is disturbed by a random noise with maximum amplitude $\xi$, which can be formulated as:

$$a_i(t) = a_i^* + \xi \cdot U(-1, 1) \tag{21}$$

where $a_i^*$ is the constant activation of muscle $i$ used in optimization and $U(-1, 1)$ is a uniform distribution in the range of [–1). Different amplitudes of noises are compared in the experiments. Starting from the same position, 100 motion experiments are conducted on the robot. The statistic index of the experiments can be found in Table 4 and the movement trajectories disturbed by different amplitude noises are sketched in Figure 6.

According to the data in Table 4, with the increase of the noise amplitude, the mean value of PE is increasing slightly, but the motion accuracy is still kept at a high level. It indicates that the CFF possesses strong robustness to noise. It can maintain the ability to constrain the robot accurately moving to the target position under the disturbance of noise.

As shown in Figure 6, when the amplitude of the noise increases, the movement trajectory of the robot in the CFF becomes unsmooth and the jitter is enhanced. However, the motion trend of the system can still approach the target point gradually along the trajectory without noise. This phenomenon is similar to a bean falling into a bowl with a bumpy surface. Although the bean will bounce in the bowl, the environmental constraints formed by the bowl will still make the bean fall to the bottom. Similarly, when the muscle activation is disturbed by random noise, although the terminal force of the robot at different positions of the CFF is disturbed, for the CFF as a whole, noise at different positions is approximately counteracted by accumulation. So the system can maintain a stable tendency of the movement. But the noise disturbance at the end of the movement has a great influence on the PE of the system.

To sum up, the CFF has a strong robustness to the noise disturbance of muscle activation. It can help the robot system to keep the movement trend stable and reach the target position with high precision, even the control precision is limited.

**Figure 6** Experiments for validating the noise robustness

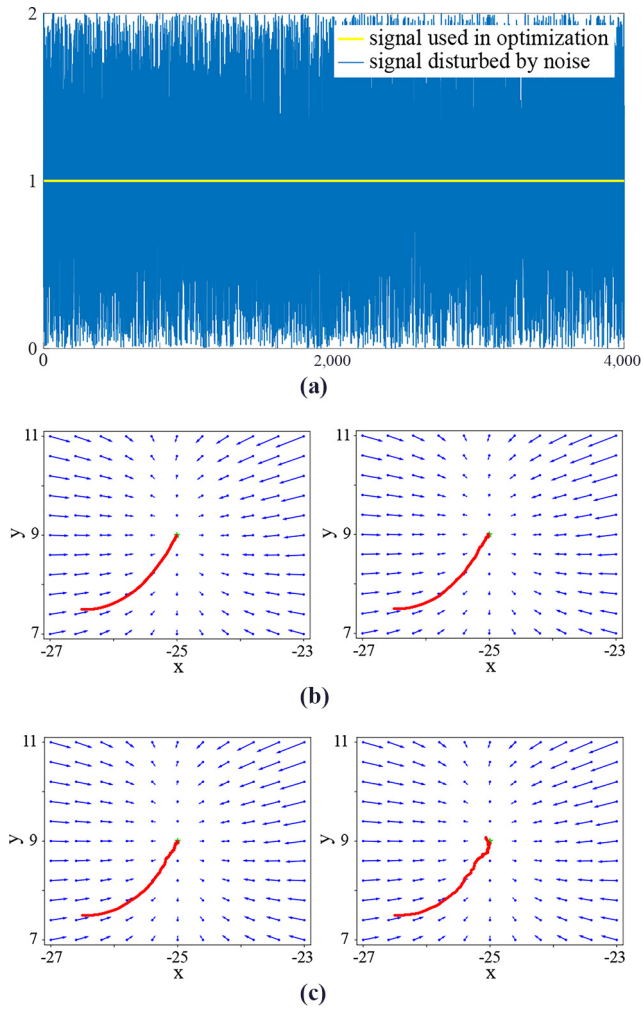


**Notes:** (a) The control signal is disturbed by noise whose amplitude is j = 1. (b)-(e) are the movement trajectories of the robot with noise amplitude j = 0.1, 0.3, 0.5, 1, respectively

### 4.4 Structure sensitivity

The CFF is constructed by optimizing the muscle arrangements. Compared with traditional articulated robots that are driven by a large electrical motor, the muscle actuator of the musculoskeletal robot is lightweight and easy to adjust, which is an important prerequisite for structure optimization.

**Table 4** Statistic index of noise robustness

| Noise amplitude | Ratio (%) | Min PE (mm) | Max PE (mm) | Mean PE (mm) | Std PE (mm) |
|---|---|---|---|---|---|
| $\xi = 0.1$ | 10 | 0.095 | 0.542 | 0.293 | 0.170 |
| $\xi = 0.3$ | 30 | 0.103 | 0.587 | 0.302 | 0.148 |
| $\xi = 0.5$ | 50 | 0.111 | 0.548 | 0.380 | 0.154 |
| $\xi = 1$ | 100 | 0.236 | 0.681 | 0.451 | 0.144 |

**Table 5** Statistic index of structure sensitivity

| Arrangements precision (mm) | Min PE (mm) | Max PE (mm) | Mean PE (mm) | Std PE (mm) |
|---|---|---|---|---|
| $10^{-3}$ | 0.086 | 0.531 | 0.260 | 2.4e−4 |
| $10^{-2}$ | 0.382 | 0.388 | 0.386 | 1.95e−4 |
| $10^{-1}$ | 1.013 | 1.020 | 1.018 | 1.9e−4 |
| 1 | 2.022 | 2.040 | 2.027 | 4.9e−4 |

In this paper, the interior point method is applied to solve the structure transforming optimization problem (11). However, the optimal solution often contains multiple decimal places. Multiple decimal places represent a high precision of muscle arrangements. This is allowed in theoretical analysis, but can not be ignored in practical system implementation. If the requirement of the muscle arrangements' accuracy is very high, it would be difficult for the physical system to realize. Hence, we discuss the influence of structure precision on the CFF in this part.

The experiments are conducted in the CFF centered with $\mathbf{r}_T = (-25, 9)$. The motion performances of the robot in the CFF with different arrangements precision are compared. As mentioned above, a $2 \times 2$ cm rectangle is adopted to illustrate the experiment result. $N_S = 100$ positions are randomly selected as the starting points of the musculoskeletal robot. The statistic index of experiments can be found in Table 5 and the movement trajectories are depicted in Figure 7.

**Figure 7** The impact of muscle arrangements precision on the CFF

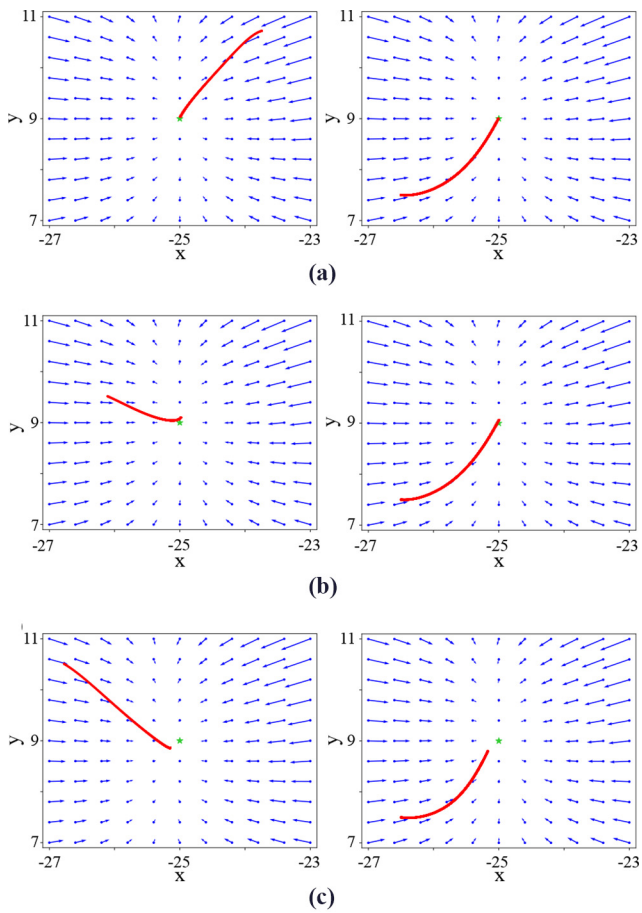


**Notes:** (a)-(c) are the movement trajectories of the robot with arrangements precision 10–2 mm, 10–1mm, 1mm, respectively

The experiment results demonstrate that with the decrease of muscle arrangement precision, the mean value of PE is increasing. It reveals that the motion performance of the musculoskeletal robot has a high sensitivity to the arrangement precision of muscle. However, it is worth noting that although the mean error of the system increase, the standard deviation of the motion error remains at a very low value. It means that although the final position of the robot at the end of the movement deviates from the target position, the robot almost always stops at the same position. So the decrease of precision of the arrangement actually causes the shift of the equilibrium center of the CFF, i.e. deviating from the original target position. But the robot can still move to the new equilibrium center with high precision under the constraint of the CFF.

## 5. Discussions and conclusions

The motivation of this paper mainly comes from the equilibrium point hypothesis in neuroscience. We proposed a structure transforming optimization algorithm for constructing CFF in musculoskeletal robotic systems. The CFF, centered with specified target positions in the task space of the robot, can be formed by optimizing the arrangements of muscles. It can help the robot move to the target position with high precision. Lyapunov stability theory is applied to analyze the condition for the robot stably reaching the target with the help of the CFF. Experiments are conducted to evaluate the performance of the proposed method in movement accuracy, noise robustness and structure sensitivity. The results demonstrate that the CFF possesses strong robustness to the noise disturbance, which lays the foundation for a robot to realize high-precision movement with limited-precision control.

CFF proposed in this paper is inspired by the convergent force field found in neuroscience and the attractive region in the environment found in information science. They are closely related but very different.

Convergent force field in the organism is formed by synergistic contractions of muscle (Bizzi *et al.*, 1991; Giszter *et al.*, 1993). In previous research of neuroscience, a few convergent force fields with equilibrium points are found in some specific positions of the limb's workspace. In this paper, by optimizing the structure of muscle arrangement, the equilibrium point of CFF can be set in plenty of different given positions of robotic workspace, which effectively expands its application range in robotics.

ARIE widely exists in the configuration space of robotic manipulation (Qiao *et al.*, 2015; Li and Qiao, 2019). It is an infeasible region in the configuration space of the robot due to

obstacles or constraints of operation objects (such as the constraints of the edge of the hole on the peg in the peg-in-hole assembly task). When the constraint region containing a unique extreme point is formed in the feasible region, the resulting "environmental attraction region" can make use of state-independent control inputs to reach the position state corresponding to the unique extreme point of the system, so as to eliminate errors caused by imprecise sensing. Therefore, the ARIE is essentially the "passive constraint" formed by the objective environment to help the robot achieve accurate movement and operation.

Compared with ARIE in robotic manipulation, which leverages the constraint formed by the operation task passively, CFF is constructed by optimizing the arrangement of muscle, which is able to actively form a constraint to help complete the given task accurately with state-independent control (i.e. the constant control signal). This capability is of great significance for robots to complete elaborate manipulation under the condition of uncertainty, such as assembly and grasping tasks in complex situations.

In the future, for extending the proposed method to practical application, we will further ameliorate the structure sensitivity of the CFF by improving the optimization algorithm. Besides, a hardware platform with a variable structure will be designed and constructed to evaluate the performance of the proposed method in a real system.

## References

Bizzi, E., Mussa-Ivaldi, F. and Giszter, S. (1991), "Computations underlying the execution of movement: a biological perspective", *Science*, Vol. 253 No. 5017, pp. 287-291.

Bizzi, E., Saltiei, P. and Tresch, M. (1998), "Modular organization of motor behavior", *Zeitschrift Für Naturforschung C*, Vol. 53 Nos 7/8, p. 510.

Bizzi, E., Accornero, N., Chapple, W. and Hogan, N. (1982), "Arm trajectory formation in monkeys", *Experimental Brain Research*, Vol. 46 No. 1, pp. 139-143.

Chen, J. and Qiao, H. (2020), "Muscle-synergies-based neuromuscular control for motion learning and generalization of a musculoskeletal system", *IEEE Transactions on Systems, Man, and Cybernetics: Systems*, pp. 1-14.

Chen, J., Zhong, S., Kang, E. and Qiao, H. (2019), "Realizing human-like manipulation with a musculoskeletal system and biologically inspired control scheme", *Neurocomputing*, Vol. 339, pp. 116-129.

Dong, H., Figueroa, N. and Saddik, A.E. (2015), "Adaptive' load-distributed' muscle coordination method for kinematically redundant musculoskeletal humanoid systems", *Robotics and Autonomous Systems*, Vol. 64, pp. 59-69.

Georgopoulos, P., A. (1994), "New concepts in generation of movement", *Neuron*, Vol. 13 No. 2, pp. 257-268.

Gilli, M., Lumia, R. and Pastorelli, S. (2014), "Precision robotic assembly using attractive regions", *International Journal of Recent Advances in Mechanical Engineering*, Vol. 3 No. 3, pp. 109-128.

Giszter, S., Mussa-Ivaldi, F. and Bizzi, E. (1993), "Convergent force fields organized in the frog's spinal cord", *The Journal of Neuroscience*, Vol. 13 No. 2, pp. 467-491.

Hart, C.B. and Giszter, S.F. (2010), "A neural basis for motor primitives in the spinal cord", *Journal of Neuroscience*, Vol. 30 No. 4, pp. 1322-1336.

Holzbaur, K.R., Murray, W.M. and Delp, S.L. (2005), "A model of the upper extremity for simulating musculoskeletal surgery and analyzing neuromuscular control", *Annals of Biomedical Engineering*, Vol. 33 No. 6, pp. 829-840.

Huang, X., Wu, W., Qiao, H. and Ji, Y. (2018), "Brain-inspired motion learning in recurrent neural network with emotion modulation", *IEEE Transactions on Cognitive and Developmental Systems*, Vol. 10 No. 4, pp. 1153-1164.

Huang, Y., Zheng, Y., Wang, N., Ota, J. and Zhang, X. (2020), "Peg-in-hole assembly based on master-slave coordination for a compliant dual-arm robot", *Assembly Automation*, Vol. 40 No. 2, pp. 189-198.

Huang, B., Zhou, M., Wang, C., Abusorrah, A. and Al-Turki, Y. (2021), "Deadlock-free supervisor design for robotic manufacturing cells with uncontrollable and unobservable events", *IEEE/CAA Journal of Automatica Sinica*, Vol. 8 No. 3, pp. 597-605.

Kargo, W.J. and Giszter, S.F. (2000a), "Afferent roles in hindlimb wipe-reflex trajectories: free-limb kinematics and motor patterns", *Journal of Neurophysiology*, Vol. 83 No. 3, pp. 1480-1501.

Kargo, W.J. and Giszter, S.F. (2000b), "Rapid correction of aimed movements by summation of force-field primitives", *The Journal of Neuroscience*, Vol. 20 No. 1, pp. 409-426.

Li, R. and Qiao, H. (2019), "A survey of methods and strategies for high-precision robotic grasping and assembly tasks–some new trends", *IEEE/ASME Transactions on Mechatronics*, Vol. 24 No. 6, pp. 2718-2732.

Li, X., Qian, Y., Li, R., Niu, X. and Qiao, H. (2020), "Robust form-closure grasp planning for 4-pin gripper using learning-based attractive region in environment", *Neurocomputing*, Vol. 384, pp. 268-281.

Liggett, B., Psuty, N.P. and Goray, E. (2010), *Kinesiology of the Musculoskeletal System*, St. Louis, Mosby/Elsevier,

Michael, G., Richard, I., George, M. and Neuroscience, C. (2009), *The Biology of the Mind*, 2nd ed., St. Louis, Mosby/Elsevier,

Millard, M., Uchida, T., Seth, A. and Delp, S.L. (2013), "Flexing computational muscle: modeling and simulation of musculotendon dynamics", *J Biomech Eng*, Vol. 135 No. 2.

Peng, G., Chen, C.L.P. and Yang, C. (2021), "Neural networks enhanced optimal admittance control of robot-environment interaction using reinforcement learning", *IEEE Transactions on Neural Networks and Learning Systems*, pp. 1-11.

Qiao, H. (2000), "Attractive regions in the environment [motion planning]", *in* IEEE International Conference on Robotics and Automation, Vol. 2, pp. 1420-1427.

Qiao, H., Chen, J. and Huang, X. (2021), "A survey of brain-inspired intelligent robots: integration of vision, decision, motion control, and musculoskeletal systems", *IEEE Transactions on Cybernetics*, pp. 1-14.

Qiao, H., Wang, M., Su, J., Jia, S. and Li, R. (2015), "The concept of' attractive region in environment' and its application in high-precision tasks with low-precision systems", *IEEE/ASME Transactions on Mechatronics*, Vol. 20 No. 5, pp. 2311-2327.

Shen, Z., Tan, L., Yu, S. and Song, Y. (2021), "Fault-tolerant adaptive learning control for quadrotor uavs with the time-varying cog and full-state constraints", *IEEE Transactions on Neural Networks and Learning Systems*, pp. 1-13.

Su, J., Hong, Q., Liu, C. and Ou, Z. (2012), "A new insertion strategy for a peg in an unfixed hole of the piston rod assembly", *The International Journal of Advanced Manufacturing Technology*, Vol. 59 Nos 9/12, pp. 1211-1225.

Wang, S., Housden, J., Bai, T., Liu, H., Back, J., Singh, D., Rhode, K., Hou, Z.G. and Wang, F.Y. (2021), "Robotic intra-operative ultrasound: virtual environments and parallel systems", *IEEE/CAA Journal of Automatica Sinica*, Vol. 8 No. 5, pp. 1095-1106.

Zhong, S., Chen, J., Niu, X. and et al (2019), "Reducing redundancy of musculoskeletal robot with convex hull vertexes selection", *IEEE Transactions on Cognitive and Developmental Systems*, Vol. 12 No. 3, pp. 601-617.

## Corresponding author

**Shanlin Zhong** can be contacted at: zhongshanlin2016@ia.ac.cn